Multiprotonation of Benzene: A Theoretical Study

Raman Sumathy*,† and Eugene S. Kryachko‡,§

Lehrstühl für Theoretische Chemie, Universität Bonn Wegelerstrasse 12, D-53115 Bonn, Germany, and Department of Chemistry, University of Leuven, Celestijnenlaan 200 F, B-3001 Leuven, Belgium

Received: May 30, 2001; In Final Form: November 12, 2001

The lower-energy portion of the potential energy surfaces of the multiprotonated benzenes are thoroughly studied at the MP2(full)/6-311++G(d,p) computational level. It is shown together with its monoprotonation results, which are well studied both experimentally and theoretically, that benzene admits di- and even triprotonation whereas the tetra one destabilizes it by opening the benzene ring. In particular, the search of the potential energy surface of the monoprotonated benzene reveals few subtle structures related to the two protonation channels, viz., $C_6H_6 + H^+ \rightleftharpoons C_6H_7^+$ and $C_6H_6 + H^+ \rightarrow C_6H_5^+ + H_2$, reported in the present work for the first time. In the former reaction, the benzenium cation may exist in two conformers. The most stable conformer is the canonical C_{2v} conformer involving σ-type of bonding. The second one, bicyclo[3.1.0] hexenyl cation, is less stable by 18.14 kcal/mol. The former conformer is separated from the van der Waals complex by the transition structure $[BzH^+]^{tr}$, wherein the excess proton is at a distance of ∼3.18 Å away from the nearest carbon atom of benzene. The other reaction channel related to the H_2 loss is underlied with two new structures. It is also found that the affinity of benzene to bind two excess protons is larger than its proton affinity by 36.9 kcal/mol. Seven lower-energy stable structures are identified in the present work on the potential energy surface of diprotonated benzene together with the transition and second-order saddle structures governing the single proton and diproton migration over the benzene ring. The lower energy portion of the triprotonated benzene consists of three minimum-energy structures, which demonstrates that the triprotonation of benzene must proceed simultaneously. An attempt has been made to characterize the vibrational spectra of protonated benzenes, which might facilitate their experimental detection.

1. Introduction

Benzene is one of the most thoroughly studied molecules. Its protonation is actually a classical example for the electrophilic aromatic substitution,[1−9] which has been a subject of enormous experimental[1−3,6−8] and theoretical studies [5,6,9,10] during the last half of the last century. The experimental proton affinity (PA) of benzene has been varied from 178.8 kcal/mol[8a] and 183 ± 3 kcal/mol[8b] to 186 kcal/mol,[8c] and it has recently been suggested to be 180.0 kcal/mol[8d] and 179.3 kcal/mol.[8e] Benzene (Bz) binds an excess proton forming the so-called benzenium ion BzH^+, which was thought[1−9] to exist in the following three conformers: (a) a face-protonated conformer with the proton residing on the C_{6v} axis; (b) a methylene-type conformer of the C_{2v} symmetry with the proton bonded to the carbon and lying out of the benzene ring; (c) an edge-type conformer with the proton perpendicular to the ring plane and being equidistantly away from the two adjacent carbon atoms of the ring.

Experiments[1−3] and theoretical studies[5,6,9,10] have shown that the methylene-type σ-conformer (b) is the most stable one. For instance, at the second-order Møller−Plesset perturbation theory (MP2) level, its proton affinity varies from 184.6 kcal/mol[9a] (MP2/4-31G(d); see also ref 6, p 311, Table 6.74) to 182.9 kcal/mol (MP2/6-31G(d))[5b] and, finally, to 178.6 kcal/mol at the compound G2(MP2(full))/6-31G(d) computational level[10e] (see also Table 1 in ref 10 g). Recently, its stability has been confirmed in the collision-induced dissociation mass spectrometry experiments on BzH^+ and BzH^+-d_6.[3a] The efficiency of loss of H and H_2 from BzH^+ has also been investigated in these experiments[3a] where the appearance of the high H-loss peak in the spectrum of BzH^+-d_6 has been interpreted due to the existence of two distinguishable isomers of BzH^+. One of them has been suggested to be a σ-type (b) complex and the other one as a π-conformer (a). This π-conformer has been estimated to be more stable than (b) with a corresponding energy difference of ∼3.5 kcal/mol. Nevertheless, its existence as a stable conformer has been ruled out in the recent theoretical G2(MP2) studies of BzH^+,[10e] demonstrating that it is actually the second-order saddle point lying above (b) by 84.5 kcal/mol at the MP2/4-31G(d)[10c] and 47.6 kcal/mol at the G2(MP2)[10e] levels (see also refs 3f and 3i−j for current reviews).

The edge-protonated conformer (c) of the C_s symmetry is actually the transition structure for the intramolecular 1,2-proton migration between the adjacent carbon atoms in Bz. The activation barrier height of this reaction falls into the interval of 7.2−9.6 kcal/mol determined via the NMR experiments in solution,[1d,2c,3i−j] and its theoretical estimation varies from ∼1 to 20.6 kcal/mol depending on the level of treatment.[9d,10a,10e−g]

The present work aims to study the multiple protonation of Bz, in parallel with the mass spectrometry experiments reviewed recently in ref 11 (see also references therein) where they appear at low abundance. Although its monoprotonation is a well

* Corresponding author. Present address: Department of Chemical Engineering Massachusetts Institute of Technology, Cambridge MA 02139. Telephone: (617) 253-6554. Fax: (617) 252-1651. E-mail: sumathy@MIT.EDU

† Universität Bonn Wegelerstrasse.

‡ University of Leuven.

§ On leave from Bogoliubov Institute for Theoretical Physics, Kiev, 03143 Ukraine.

10.1021/jp012052w CCC: $22.00
Published on Web 12/27/2001

studied subject, as presented above, we intend to enrich our knowledge of the lower-energy portion of its potential energy surface (PES). The primary goal of the present work is to show that benzene admits diprotonation and triprotonation, and its simultaneous diprotonation is even more energetically favorable compared to its monoprotonation in the sense that the diproton affinity of benzene exceeds its proton affinity by about 20%. The PES of the diprotonated Bz includes stable structures of both σ and π bonding. It is also demonstrated that the tetra protonation of benzene leads to its destabilization via a ring opening.

2. Computational Strategy

A rather exhaustive search of the PESs of the mono-, di-, and triprotonated Bz was performed at the MP2(full) computational level with the 6-311++G(d,p) basis set using the GAUSSIAN 98 suit of packages.[12] Such a computational level is found to describe adequately the ground-state of the benzene molecule. The calculated C−C bond length is equal to 1.4002 Å and the C−H bond length is 1.0867 Å, which is in rather good agreement with the latest experimental (1.3902 ± 0.0002 and 1.0862 ± 0.0015 Å, respectively) findings[13a] and the high-level MP2(full)/TZ2P+f computational data (1.3896 and 1.0804 Å, respectively).[13b] The extreme energy points on the PESs of the mono-, di-, and triprotonated Bz were further characterized by its harmonic force constants calculated at the MP2 (frozen core ≡ fc)/6-31G(d,p) level. The harmonic frequencies and zero-point vibrational energies (ZPVE) were retained unscaled. At this computational level, the six harmonic C−H stretching vibrations of Bz were calculated at 3249 cm^{-1} (B_1 symmetry, 7 km/mol; 3057 cm^{-1}; 3172.0 cm^{-1}), 3259 cm^{-1} (E_2, 7 km/mol; 3056.7 cm^{-1}; 3191 cm^{-1}), 3274 cm^{-1} (E_1, 36 km/mol; 3064.367 cm^{-1}; 3191 cm^{-1}), and 3284 cm^{-1} (A_1, 7 km/mol; 3073.942 cm^{-1}; 3208 cm^{-1}). The numbers in parantheses correspond to the irreducible representation of the vibration within the D_{6h} point group, the corresponding to theoretical IR intensities, and the gas-phase experimental frequencies[13c] followed by the theoretical ones.[13b,d] The five C=C stretching vibrations of Bz were the following: 1396 cm^{-1} (A_{2g} symmetry (see ref 13e), 0 km/mol; 1309.4 cm^{-1}; 1461 cm^{-1}), 1541 cm^{-1} (E_{1u}, 8 km/mol; 1483.985 cm^{-1}; 1515 cm^{-1}), 1674 cm^{-1} (E_{2g}, 0 km/mol; 1600.976 cm^{-1}; 1637 cm^{-1}), with similar data within parantheses as for the aforementioned ν(C−H) stretching modes.

Throughout the present work, the energy comparison was made in terms of the electronic energy at the MP2(full)/6-311++G(d,p) level with ZPVE corrections at the MP2(fc)/6-31G(d,p) level unless otherwise notified.

3. Potential Energy Surface of Monoprotonated Benzene

The process of protonation of benzene is studied by approaching the excess proton H^+ from infinity to Bz in two different ways associated with the following reaction channels:

$$C_6H_6 + H^+ \rightleftharpoons C_6H_7^+ \quad (1)$$

and

$$C_6H_6 + H^+ \rightarrow C_6H_5^+ + H_2 \quad (2)$$

The former channel (1) involves the association of H^+ leading to the benzenium cation while the latter (2) describes the H_2 loss[3a] wherein the excess proton attacks collinearly the C−H bond of bare benzene. Channel (2) does not have any precursor state. The channel (1) includes a van der Waals complex (vdW) that is separated from the benzenium cation (b) by the transition state $[BzH^+]^{tr}$ with a distance of ~3.18 Å between the excess proton H^+ and the contiguous carbon atom C_1 of Bz (see Figure 1).[14] Channel (1) also includes a new structure ($\tilde{b}$). We consider (b) and ($\tilde{b}$) below and turn now to the transition structure $[BzH^+]^{tr}$ reported for the first time.

$[BzH^+]^{tr}$ is placed below the asymptote Bz + H^+ by 82.40 kcal/mol. This is shown in Figure 1. Notice that due to the fact that the ionization energy of benzene is equal to 9.24378 eV, this asymptote lies beneath the ground-state asymptote Bz^+ + H by 15.47 kcal/mol. Owing to the large difference in the entropies of the reactants (bare benzene and the proton) and $[BzH^+]^{tr}$, the free energy difference between $[BzH^+]^{tr}$ and the asymptote Bz + H^+ reaches 90.57 kcal/mol at room temperature. As a transition structure, $[BzH^+]^{tr}$ is characterized by an imaginary frequency of 607 cm^{-1} assigned to the coupled C_1−H_1 and C_1−H^+ stretching modes. Despite the excess proton being far away from the benzene ring, as seen in Figure 1, it nevertheless affects the structure of Bz quite substantially. Namely, the two C−C bonds adjacent to the carbon atom, C_1, closest to the excess proton are elongated by 0.025 Å, the second-neighbor C−C bonds are shrunk by nearly the same amount, and the next-neighbor bonds are elongated by 0.028 Å. The hydrogen atom H_1 forming the C−H bond with the carbon atom C_1 moves slightly downward by 5.2° with respect to the Bz ring. The angle between the excess proton and the C_1−H_1 bond is found to be 53.8°. All C−H stretching vibrations of the transition structure $[BzH^+]^{tr}$ are blue-shifted by 10−15 cm^{-1} compared to that of bare benzene and their IR intensities are suppressed except for the C_1−H_1 stretching vibration whose IR intensity increases by a factor of nearly 4.

Within the MP2(full)/6-311++G(d,p) level, the lower-energy portion of the PES of the monoprotonated Bz is described by two reaction channels, (1) and (2). It is composed of three minima, three transition structures including the aforementioned transition structure $[BzH^+]^{tr}$, two saddle points of second order, and one saddle point of third order. One of these minima and one second-order saddle point are referred to the channel (2), while the remainder of the extreme-energy structures are referred to channel (1). All these structures are depicted in Figure 1.

The global minimum is achieved at the classical structure (b) of the C_{2v} symmetry with a nearly tetrahedral protonation site at C_1 (see Figure 1). The protonation of bare benzene causes the elongation of the C−H bonds at this site by ~0.02 Å and of the adjacent C−C bonds by ~0.07 Å, whereas the second-neighbor C−C bonds are shortened by ~0.02 Å and, vice versa, the third-neighbor bonds become also elongated by ~0.01 Å. Table 1 demonstrates a fair agreement between theoretical and experimental geometries of the monoprotonated Bz. As shown in Table 2, the protonation of benzene accumulates the positive Mulliken charge on the carbon atom C_1 at the protonation site.

The energy difference between the stable benzenium ion and Bz that is actually the PA of bare benzene amounts to 180.14 kcal/mol at the MP2(full)/6-311++G(d,p) and 179.66 kcal/mol at the MP2(fc)/6-31G(d,p) level after ZPVE correction. The agreement with the earlier theoretical results[10e,g] is rather very good. The enthalpy of formation of benzenium at 298.15 K is 179.27 kcal/mol. The latter is also in a fair accordance with the recently reported experimental proton affinity of 180 kcal/mol.[8d] Relative to the transition structure $[BzH^+]^{tr}$, the benzenium structure (b) lies below it by 90.86 kcal/mol (Figure 1). With regard to the C−H stretching vibrations, the protonation of Bz red-shifts them by ~200 cm^{-1} and enhances the stretching vibrations of the C−H bonds at the protonated site. Comparing

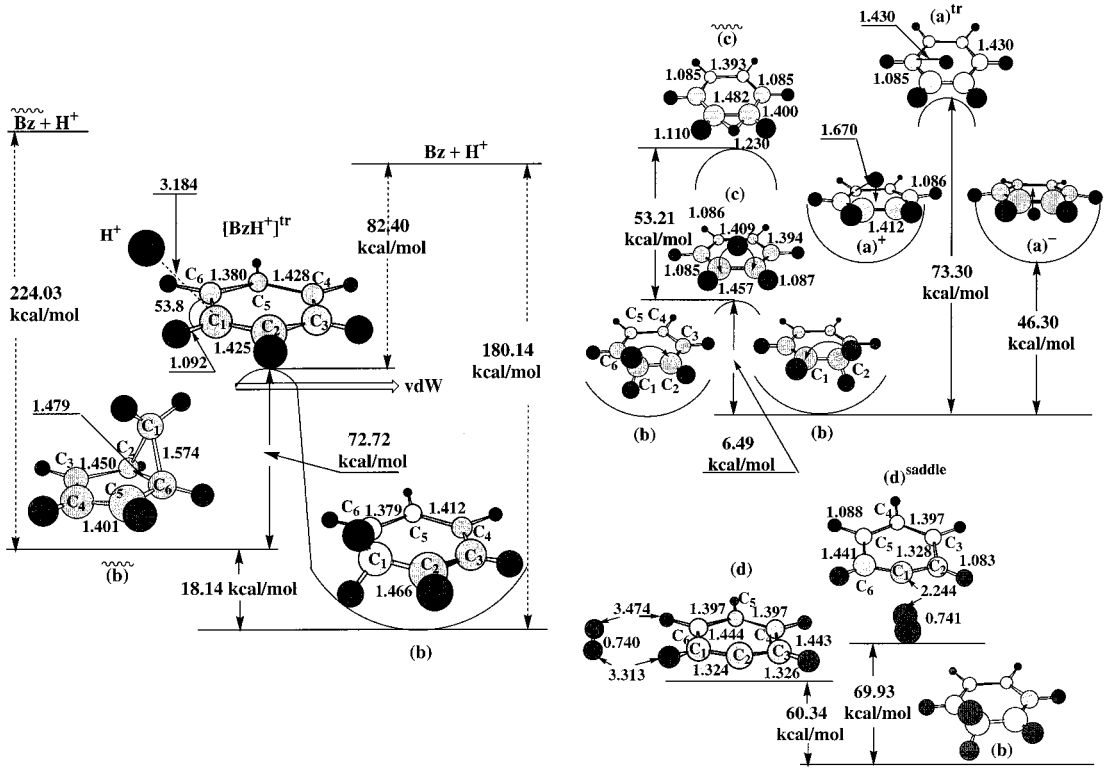

Figure 1. Lower energy portion of PES of monoprotonated benzene. The carbon atoms are shown by light circles while the hydrogen atoms by the dark ones. The PAs of the Bz and $\widetilde{Bz}$ are taken at the MP2(full)/6-311++G(d,p) computational level without ZPVE. Bond lengths in Å, bond angles in deg. Dashed arrows indicate the unscaled relative energy difference. Double arrow shows the reaction path from the transition structure $[BzH^+]^{tr}$ to the vdW complex.

TABLE 1: Geometries of Some Extremum Energy Structures on the PES of BzH^+,[a]

$C_6H_7^+$ geometry	$BzH^{+,theor}$ (b)	$BzH^{+,expt[5a]}$	$BzH^{+,theor}$ (b)	(d)	$(d)^{saddle}$
$r(C_1C_2)$	1.466 (1.464)[b]	1.490	1.574	1.324	1.328
$r(C_2C_3)$	1.379 (1.375)[b]	1.365	1.450	1.326	1.441
$r(C_3C_4)$	1.412 (1.406)[b]	1.407	1.401	1.443	1.397
$\angle C_2C_1C_6$	117.6 (117.3)[b]	115.4	56.0	102.7	148.1
$\angle C_1C_2C_3$	120.6 (120.8)[b]	121.1	107.5	149.3	103.4
$\angle C_2C_3C_4$	119.0 (119.0)[b]	119.6	110.3	103.0	122.0
$\angle C_3C_4C_5$	123.1 (123.0)[b]	122.8	107.9	122.0	120.8

[a] For enumeration of the atoms see Figure 1. Bond lengths in Å, bond angles in deg. [b] MP2(full)/6-31G(d) results (ref 10e.

with the C−H stretching vibrations of bare benzene mentioned in section 2, the harmonic stretching vibrations of these C−H bonds of the benzenium cation appear at 3037 (80 km/mol; symmetric) and 3059 (33 km/mol; asymmetric) cm^{-1}. Its remaining ν(C−H) modes are collected in Table 3. Among the ν(C−C) modes of the benzenium cation, it is interesting to mention that their lowest mode absorbs at 1387 cm^{-1} and it corresponds to the C−C stretch of the bonds adjacent to the protonation site. Comparing with the stretch of Bz with absorptions at 1396 cm^{-1}, this blue-shift can easily be correlated with their lengthening mentioned above. The most IR active ν(C−C) vibration is calculated at 1580 cm^{-1} with the IR intensity equal to 178 km/mol. It describes the coupled symmetric stretching vibration of the bonds between the second and the third neighboring carbon atoms with respect to the protonation site.

To resolve the longstanding perplexing controversy on the existence of another stable π structure of the benzenium (see, e.g., refs 15,3a,10c, and 10e) which, according to refs 15 and 10c, may only be considered as a transition structure, we perform a rather exhaustive search of the lower-energy portion of the PES of BzH^+. This search leads us to another structure with a broken C_{2v} symmetry that is partly attributed to π bonding and absolutely isoenergetic to the structure (b). However, subsequent optimization of this complex using the tight criteria results precisely in (b). Another possible explanation of the appearance of the π-benzenium with a finite lifetime has been recently proposed in ref 16.

The 1,2-migration of the excess proton from one carbon atom to the adjacent one occurs via two different paths. We envision one of them as passing through the transition structure (c) of the C_s symmetry shown in Figure 1. At the MP2(full)/6-311++G(d,p) level, it lies by 6.49 kcal/mol above the linked global minima of the (b) type. This value increases to 7.86 kcal/mol at the MP2(fc)/6-31G(d,p) level and lowers to 6.28 kcal/mol after ZPVE correction (cf. refs 10e−h; see also refs 3f and 3i−j for current reviews). Due to the entropy excess of the (b) minimum over the (c), the free energy of the proton migration reaches 6.68 kcal/mol at room temperature, which is in a satisfactory agreement with the activation free energy of 8.0 ± 1 kcal/mol measured by Olah et al.[1d] The bridged proton resides by ∼1.03 Å above the Bz ring and is equidistant from the nearest carbon atoms by 1.305 Å and forms a bond angle of 56.0° with the two adjacent carbon atoms. Such a rather small barrier height of the 1,2-migration of the excess proton arises apparently due to its attraction to the π electronic cloud of the Bz ring and may lead to the "proton ring walk".[3j] The magnitude of the imaginary frequency related to the activation barrier is equal to 398 cm^{-1} and it corresponds to the normal mode describing the proton migration between the relevant C atoms.

The other path of the 1,2-proton migration between the adjacent carbon atoms occurs throughout the Bz plane. It is governed by the transition state (c) displayed in Figure 1. The excess proton resides in the Bz plane with a distance of 1.23 Å

TABLE 2: Mulliken Charges (in a.u.) of the Minimum Energy Structures of the *n*-Protonated Bz ($1 \le n \le 3$)[a]

atom	(b)	(m)	(o)	(p)	(p^{π})	$(b)_3^1$	$(b)_3^2$
C_1	0.077	1.021	0.460	0.361	0.096	1.775	1.097
C_2	−0.076	−0.909	−0.152	0.360	0.098	−2.166[b]	−0.412
C_3	0.054	1.021	−0.151	−1.345[b]	−0.671[b]	1.775	0.478[b]
C_4	−0.076	−1.896[b]	0.461	0.360	0.099	−2.166[b]	−1.850[b]
C_5	0.077	1.635	−0.777[b]	0.361	0.096	1.775	1.625
C_6	0.283[b]	−1.896[b]	0.772[b]	−1.345[b]	−0.668[b]	−2.166[b]	−1.946[b]
H_7	0.000	0.397	0.372	0.413[b]	0.377[b]	0.495	0.443[b]
H_8	−0.003	0.363[b]	0.415	0.396	0.378	0.448[b]	0.404[b]
H_9	0.003	0.438	0.353[b]	0.396	0.378	0.495	0.483
H_{10}	−0.062[b]	0.363[b]	0.352[b]	0.413[b]	0.377[b]	0.447[b]	0.461[b]
H_{11}	0.003	0.397	0.415	0.396	0.378	0.495	0.478
H_{12}	−0.003	0.340	0.372	0.396	0.378	0.447[b]	0.428
H_{13}	0.449[b]	0.363[b]	0.325[b]	0.419[b]	0.341[b]	0.447[b]	0.462[b]
H_{14}	−	0.363[b]	0.325[b]	0.419[b]	0.341[b]	0.447[b]	0.404[b]
H_{15}	−	−	−	−	−	0.447[b]	0.443[b]

[a] Mulliken charges of Bz are: $q(C) = -q(H) = -0.195$. Location of the excess proton(s) is indicated by the superscript *b*.

TABLE 3: ν(C−H) and ν(H−H) Stretching Vibrations of the Minimum-Energy Structures of the Multiprotonated Bz

(b)	(d)	(m)
3037 (80) sym	3268 (21) sym	2926 (11) 2931 (261)
C_1-H_1, C_1-H^+	C_4-H_4, C_6-H_6	2932 (430) 2941 (36
3059 (33) asym	3271 (22) asym	all C−H at C_4, C_6
C_1-H_1, C_1-H^+	C_4-H_4, C_6-H_6	3234 (51) C_5-H_5
3270 (0.2); 3281.5 (3)	3308 (22) C_5-H_5	3255.6 (5) 3257.0 (69)
3282.2 (9); 3307.5 (8)	3322 (203) sym	C_1-H_1, C_3-H_3
3308.7 (2)	3326 (64) asym	3294 (58) C_2-H_2
	C_1-H_1, C_3-H_3	
	4581 (5) H−H	
(o)	**(p)**	**(p^{π})**
2818 (248) 2823 (313)	2801 (398) 2805 (0)	2574 (541) 2581 (0)
C_5-H^+, C_6-H^+	2858 (849) 2864 (0)	C_1-H^+, C_4-H^+
3038 (105) 3043 (207)	all C−H at C_3 and C_6	3183 (161) 3186 (0.5)
C_5-H_5, C_6-H_6	3253.7 (0) 3254.7 (73)	C_1-H_1, C_4-H_4
3237.6 (74) sym 3237.9 (2) asym	3262 (202) 3264 (0)	3250.9 (0) 3251.7 (87)
3237.9 (2) asym	all C−H on the other carbon atoms	3259 (184) 3261 (0)
C_1-H_1, C_4-H_4		all C−H on the other carbon atoms
3264 (36) 3272 (75)		
C_2-H_2, C_3-H_3		
$(d)_2^1$	**$(d)_2^2$**	**$(b)_3^1$**
2356 (68) 2631 (192)	3119 (347) C_1-H_1	2759 (0) 2759 (0)
C_1-H_1 $C_1-H_a^+$	3157 (138) 3164 (118)	2766 (760) 2800 (739)
2848 (219) $C_1-H_a^+$	C_3-H_3, C_4-H_4	2800 (739) 2820 (0)
3257 (10) C_4-H_4	3160 (153)	all C−H at C_1, C_3, C_5
3261 (54) 3263 (55)	C_4-H_4, C_6-H_6	3167 (176) 3167 (176)
C_2-H_2, C_6-H_6	3286.3 (163) 3286.8 (1)	3172 (0)
3286 (96) 3287 (26)	C_2-H_2, C_5-H_5	all C−H on the other carbon atoms
C_3-H_3, C_5-H_5	4536 (39) H−H	

[a] Frequencies in cm^{-1}, IR intensities in km/mol in parentheses. Sym and asym are the shorthand notations for the symmetric and asymmetric stretching vibrations, respectively.

to the carbon atoms involved in migration and produces the elongation of their C−C bond by 0.08 Å. The transition structure (c) lies higher than the transition structure (c) of the out-of-plane migration by 53.21 kcal/mol. The corresponding transition frequency 1536 cm^{-1} is assigned to the vibrational mode of the excess proton perpendicular to the ring.

Between the opposite protonation sites (1,4-proton migration), the excess proton probably migrates via the second-order saddle structure (a) of the C_{6v} symmetry with a proton-carbon distance of 1.67 Å (Figure 1). However, it must be stated that saddle points with a Hessian index greater than one are chemically not significant. At room temeperature, the free energy difference between (a) and (b) structures amounts to 48.95 kcal/mol. The (a) structure has the degenerate imaginary frequency 1658 cm^{-1}, which describes the motion of the excess proton parallel to the benzene ring. Actually, there are two equivalent structures of the (a) type: one, $(a)^+$, with the proton lying above the ring, and the other one, $(a)^-$, with the proton lying below it. These are demonstrated in Figure 1. We identified another saddle structure of Hessian index 3 $(a)^{tr}$ that could probably link $(a)^+$ and $(a)^-$ (Figure 1). The migrating excess proton in $(a)^{tr}$ is at the center of Bz and is energetically placed above the global benzenium structure by ~73.30 kcal/mol and characterized by three imaginary vibrational modes, viz., at 212 cm^{-1} and the doubly degenerate mode at 911 cm^{-1}. As mentioned above, a word of caution must be exercised while deriving the understanding of a chemical system through second and third-order saddle points.

The minimum energy structure ($\tilde{b}$) depicted in Figure 1 is reported in the present work for the first time. It resides on the PES of BzH^+ above the classical benzenium ion (b) by 18.14 kcal/mol. Besides, ($\tilde{b}$) can also be considered as the protonated structure of the tricylic isomer of benzene, viz., tricyclo[4.1.1.0]-pent-3-ene, named herein merely as $\widetilde{Bz}$. The details of this isomer are presented in the Appendix. Relative to ($\tilde{b}$), its PA amounts 224.03 and 214.02 kcal/mol after ZPVE. The computed

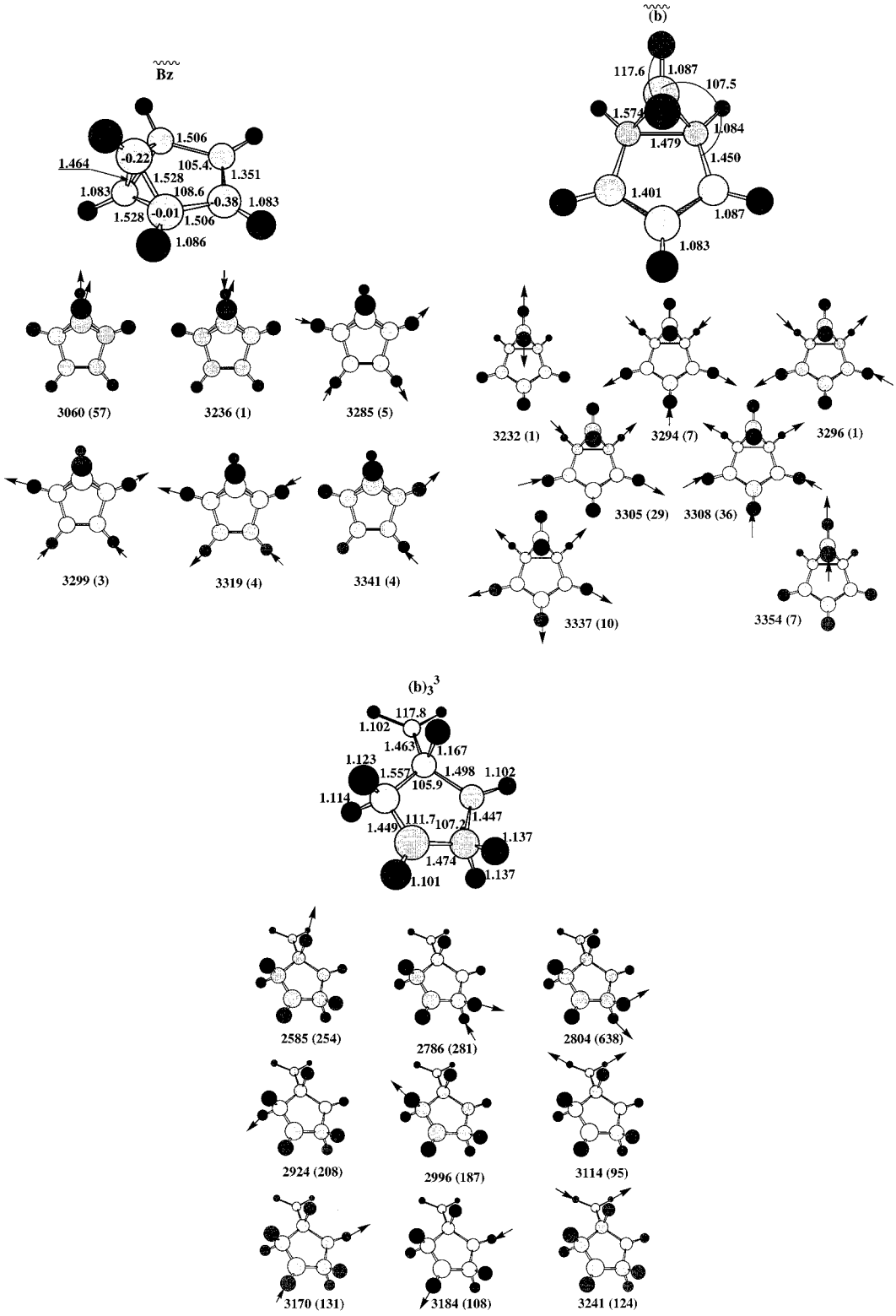

Figure 2. Tricyclic isomer of benzene $\widetilde{Bz}$ and its protonated structure ($\tilde{b}$) and the triprotonated one $(b)_3^3$: geometry, their harmonic C−H stretching vibrations, and corresponding vectors of normal displacements indicated by arrows. Mulliken charges (in a.u.) on the carbon atoms of $\widetilde{Bz}$ are also shown. The corresponding Mulliken charges in Bz are equal to $q(C) = -0.195$. Bond lengths in Å, bond angles in deg., frequencies in cm^{-1}, IR intensities in km/mol.

rotational constants of ($\tilde{b}$) are as follows: $A = 6697.1517$ (5415.0669) MHz, $B = 4806.5127$ (5300.8091) MHz, and $C = 3516.6776$ (2721.2472) MHz. The numbers in parentheses correspond to the benzenium ion given for a comparison sake. It is also interesting to compare them with the calculated rotational constants of bare benzene, viz., $A = B = 5660.5152$ MHz and $C = 2830.2576$ MHz. In Figure 2, the normal displacements of the harmonic C−H stretching vibrations of the structure ($\tilde{b}$) are pictorially displayed and compared to those pertaining to its parent molecule $\widetilde{Bz}$.

The lower-energy portion of the PES of BzH^+ referring to the reaction channel (2) consists of the second-order saddle structure $(d)^{saddle}$ and the minimum energy structure (d), both shown in Figure 1. The structure $(d)^{saddle}$ governs the dissociation

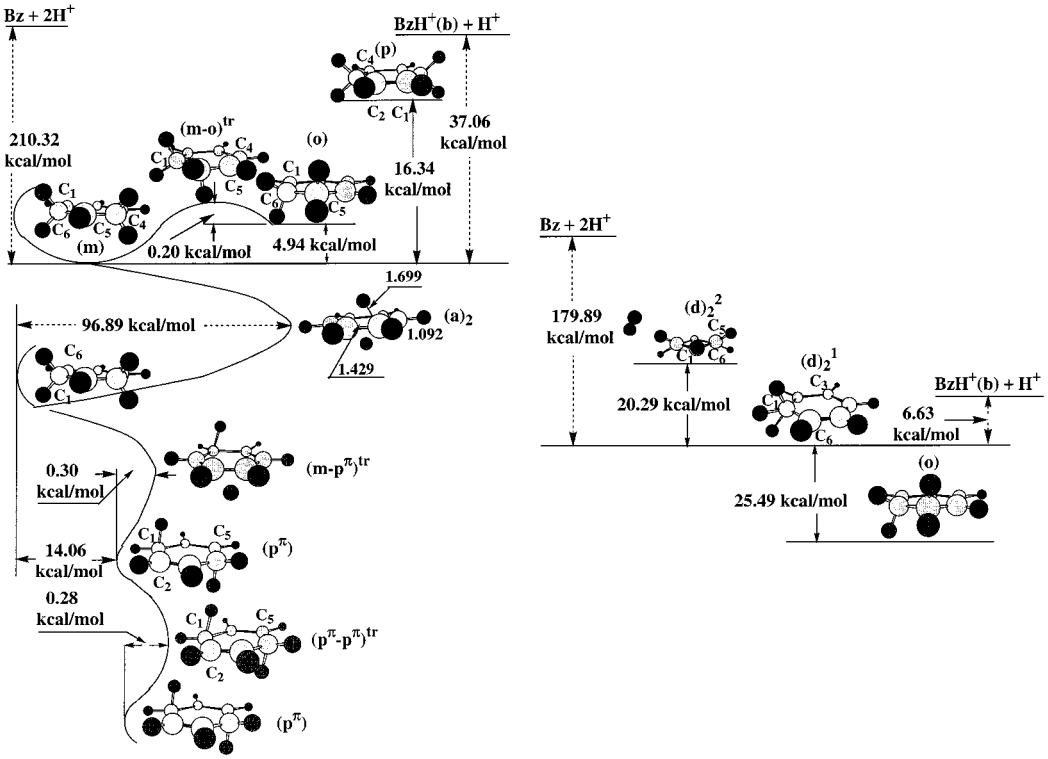

Figure 3. Lower energy portion of the potential energy surface of the diprotonated benzene. Bond lengths in Å. Dashed arrows indicate the unscaled relative energy difference.

of the benzenium cation into $C_6H_5^+$ and the H_2 molecule. It occurs when the two hydrogens of the methylene group of (b) approach each other. As shown in Figure 1, in (d)^{saddle}, the H_2 molecule with a bond length of 0.741 Å is separated by a distance of 2.244 Å from the carbon atom to which they are bonded in the reactant. The loss of H_2 shrinks the C−C bonds between this carbon atom and the adjacent ones in $C_6H_5^+$ by ∼0.07 Å and increases the related bond angle by 8°. Energetically, such a saddle point with a barrier of 69.93 kcal/mol separates the benzenium cation from the product of the reaction 2. The structure (d) resides above the benzenium cation by 69.82 kcal/mol (60.34 kcal/mol after ZPVE correction). It is structurally composed of the H_2 molecule loosely bound to the $C_6H_5^+$. The H_2 bond length is equal to 0.740 Å, which fairly well resembles the experimental equilibrium H−H distance of 0.7414 Å of the ground-state hydrogen molecule.[17] It follows from Table 3 that the H−H stretching vibration frequency of 4581 cm^{-1} predicted in the present study also agrees satisfactorily with the experimental ν(H−H) of 4400 cm^{-1}.[17]

4. Diprotonated Benzene

Unlike the lower-energy portion of the PES of BzH^+, as studied in the preceding section, where one of the pathways describes the reaction channel (1) and contains the global minimum assigned to the benzenium cation and the other one governs the reaction 2 and relates to the loosely bound complex of H_2 to $C_6H_5^+$, the PES of the diprotonated benzene displayed in Figure 3 possesses seven lower-energy minima. Three of them belong to the C_{2v} point group and resemble the benzenium cation structure with the two excess protons occupying relatively, the meta, ortho, and para orientations. The meta-diprotonated σ-type structure (m) is the global minimum of the BzH_2^{2+} PES. Its diproton affinity defined as the difference in energy between the (m) complex and that of bare benzene is equal to 210.32 kcal/mol. Therefore, the diproton affinity of benzene exceeds its proton affinity by ∼20%, implying thus that the diprotonation of benzene is actually more energetically favorable than its monoprotonation.

In Table 4 we demonstrate that the diprotonation of Bz at the meta position lengthens the neighboring C−C bonds by 0.04 and 0.08 Å. This causes a red shift ca. 15 cm^{-1} in the calculated ν(C−C) stretching vibration of the C−C bonds adjacent to the protonation sites. At the protonation sites, the bond angle ∠HCH equals 96.3°. We observe a slight symmetric distortion of this structure due to a very small inequivalence in the positioning of hydrogens at the protonation sites, which persists even after applying the tight optimization criteria. This may be attributed to some sort of π interaction leading partially to the stabilization of (m). The diprotonation of Bz at the meta position also results in the appearance of rather IR intense and quite narrow band composing of four harmonic vibrations assigned to the stretching vibrations of C−H bonds placed at the protonation sites and centered at 2926 (11 km/mol), 2931 (261 km/mol), 2932 (430 km/mol), and 2940 cm^{-1} (36 km/mol) (see Table 3). Their comparison with those of the benzenium cation shows that the diprotonation further red shifts the C−H stretching vibrations at the protonation sites by ∼111 cm^{-1}. We also observe that the diprotonation enhances and shifts the C−H stretching vibrations of the remaining sites of the (m) structure as well. Analyzing Table 2, we also conclude that the diprotonation leads to a further accumulation of the negative charge on the carbon atoms residing at the protonation sites.

The ortho structure (o) is placed above the meta structure by 4.94 kcal/mol and is followed by the para structure (p), which is even higher by 18.10 kcal/mol (16.34 kcal/mol after ZPVE) than (m) (Figure 3). Using the Mulliken charges of the meta and para structures presented in Table 2, we may simply estimate the difference between their total Coulomb energies. This estimation gives a value of 21.8 kcal/mol, which is rather close to the aforementioned value of 18.10 kcal/mol bearing in mind

TABLE 4: Geometries of Some Extremum-Energy Structures of the Diprotonated Bz[a]

geometry	(m)	(o)	(p)	(p^{π})
$r(C_1C_2)$	1.393	1.443	1.411	1.410
$r(C_2C_3)$	1.393	1.393	1.451	1.454
$r(C_3C_4)$	1.482	1.443	1.451	1.454
$r(C_4C_5)$	1.443	1.431	1.411	1.410
$r(C_5C_6)$	1.443	1.506	1.451	1.454
$r(C_6C_1)$	1.482	1.431	1.451	1.454
$r(C_1H_1)$	1.092	1.094	1.091	1.091
$r(C_2H_2)$	1.087	1.090	1.091	1.091
$r(C_3H_3)$	1.092	1.090	1.133	1.094
			-0.775^b	
$r(C_4H_4)$	1.120	1.094	1.091	1.091
	-0.830^b			
$r(C_5H_5)$	1.095	1.141	1.091	1.091
		$+1.020^b$		
$r(C_6H_6)$	1.120	1.141	1.133	1.094
	$+0.833^b$	-1.020^b	$+0.775^b$	
r(CH)[b]	1.120	1.104	1.136	1.181
	$+0.833^b$	-0.618^b	$+0.803^b$	$+1.137^b$
r(CH)[b]	1.120	1.104	1.136	1.181
	-0.830^b	$+0.618^b$	-0.803^b	-1.137^b

geometry	$(m-o)^{tr}$	$(m-p^{\pi})^{tr}$	$(p^{\pi}-p^{\pi})^{saddle}$	$(d)_2^1$	$(d)_2^2$
$r(C_1C_2)$	1.402	1.438	1.441	1.501	1.399
$r(C_2C_3)$	1.454	1.412	1.412	1.373	1.399
$r(C_3C_4)$	1.392	1.456	1.459	1.424	1.464
$r(C_4C_5)$	1.433	1.437	1.441	1.424	1.399
$r(C_5C_6)$	1.439	1.413	1.412	1.373	1.399
$r(C_6C_1)$	1.502	1.466	1.459	1.501	1.462
$r(C_1H_1)$	1.097	1.091	1.092	1.141	1.105
$r(C_2H_2)$	1.094	1.090	1.092	1.090	1.089
$r(C_3H_3)$	1.090	1.091	1.091	1.088	1.100
$r(C_4H_4)$	1.089	1.092	1.092	1.091	1.100
$r(C_5H_5)$	1.094	1.091	1.091	1.088	1.089
$r(C_6H_6)$	1.089	1.091	1.091	1.090	1.101
r(CH)[c]	1.169	1.284	1.202	1.195	3.193
r(CH)[c]	1.131	1.197	1.202	1.208	3.191

[a] For enumeration of the atoms see Figure 3. Bond lengths in Å. The superscript *b* indicates the distance above (+) and below (−) the Bz ring, respectively, and *c* the C−H bonds with the residing excess protons except the two last structures.

a crudeness of the chosen model. It is readily seen from the geometry of the ortho structure presented in Table 4 that the two excess protons reside largely above and below the Bz ring. This implies that (o) is attributed to the interaction of the excess protons with the σ and π electrons of benzene. The bond angle $\angle$HCH at the ortho protonation site is found equal to 97.7°, which reduces to 88.8° in the para structure where the excess protons are solely bonded via their interaction with the σ electrons of Bz.

The migration of one of the excess protons from the meta to the ortho orientation is governed by the transition state $(m-o)^{tr}$, whose imaginary frequency amounts to 425 cm^{-1} and describes the migration of one excess proton between the adjacent carbon atoms. This transition state is placed by ca. 0.2 kcal/mol above the ortho structure. Apparently, such a small barrier makes the ortho-diprotonated benzene rather unstable. On the other side, relative to the meta structure, the barrier is composed of ∼5 kcal/mol. Comparing it with the librational frequency of 1186 cm^{-1} of the migrated excess proton, we conclude that the first vibrational level of such librational mode lies in the vicinity of the barrier top. Thus, its population promotes a tunneling through this transition state or even the classical transition over the activation barrier resulting in a rather free migration of the excess proton between the two adjacent meta structures.

The fourth minimum (p^{π}) of the diprotonated benzene is quite remarkable. Both the excess protons reside at the opposite sides of the Bz ring, forming a bond angle of 103.6° with the corresponding C−H bonds. Thus, they are substantially π-bonded to the benzene molecule. Its analogues for the meta and ortho structures are absent. Such a π-para structure lies above the meta structure by 14.06 kcal/mol and below the canonical para structure (p) by 2.28 kcal/mol. The partly π-bonded protons are characterized by symmetric and asymmetric stretching vibrations at 2574 and 2581 cm^{-1} which are reds hifted by 609 cm^{-1} from the symmetric and asymmetric stretching vibrations of the adjacent σ-bonded hydrogens (see Table 3). Interestingly, the symmetric stretching vibration at 2574 cm^{-1} is predicted to be significantly IR active with an IR intensity of 541 km/mol. This might serve as a potential "fingerprint" in its experimental detection.

The transition structure $(m-p^{\pi})^{tr}$ with an imaginary frequency of 435 cm^{-1} governing the double proton migration from the meta- to the (p^{π}) structure is very close, by ∼0.31 kcal/mol, to the latter one. This probably affects the stability of the π-para structure relative to the meta structure. A similar activation barrier of 0.28 kcal/mol is predicted for the double proton migration of the π-diprotonated structure (p^{π}) over the benzene ring. We name it as $(p^{\pi}-p^{\pi})^{saddle}$ and display in Figure 3. Such small barriers likely make a "di-proton walk" over the benzene ring rather feasible.

It is also worth mentioning that the face-protonated structure $(a)_2$ of $C_6H_8^{2+}$ is an analogue of the (a) structure on the PES of BzH^+. It has two excess protons on the opposite sides of the Bz ring placed by 1.699 Å from the carbon atoms. The C−C distance is elongated by ∼0.03 Å relative to that in Bz. Energetically, it lies above the meta structure by 96.89 kcal/mol and is in fact a fourth-order saddle point with two doubly degenerated imaginary frequencies, 1497 and 2028 cm^{-1}, both describing the vibrations of the excess protons parallel to the Bz plane.

As we have seen in the preceding section, the PES of BzH^+ describes partially the reaction channel (2) associated with the experimentally observed loss of H_2 due to protonation of bare benzene. Based on the present analysis of the lower-energy portion of the PES of the diprotonated Bz, which reveals two additional lower-energy minima of the $(Bz + H_2)^{2+}$ type, we suggest that they may be actually linked to the reaction channels exiting with H_2. Among these two minima, the lowest structure $(d)_2^1$ shown in Figure 3 is located by 179.89 kcal/mol below the dissociative asymptote $Bz + 2H^+$. Comparing with the global minima of the mono- and diprotonated Bz, it lies below the dissociation limit (b) + H^+ by only 6.63 kcal/mol and above the ortho structure by 25.49 kcal/mol. As shown in Figure 3, in the $(d)_2^1$ structure both excess protons are bonded to the C_1-H_1 bond, causing its upward rotation out of the benzene ring by 73.5°. One of them resides almost in the ring plane while the other one lies below it. They form a sort of H_2 diatomic cation with a bond length of 1.03 Å, which is stabilized by their bonding to the carbon atom C_1. For this reason, such a structure may be referred to as a π-H_2-type conformer of the diprotonated benzene. It is rather interesting that such binding of the two excess protons to the single C−H bond manifests spectroscopically by the appearance of three rather IR active stretching vibrational modes of the C−H type, viz., 2356 (68 km/mol), 2631 (192 km/mol), and 2849 cm^{-1} (219 km/mol). The other energy-minimum structure $(d)_2^2$ partially resembles the complex (d) of the monoprotonated Bz and actually has a boat-like form (see Figure 3). It is placed above $(d)_2^1$ by 20.29 kcal/mol

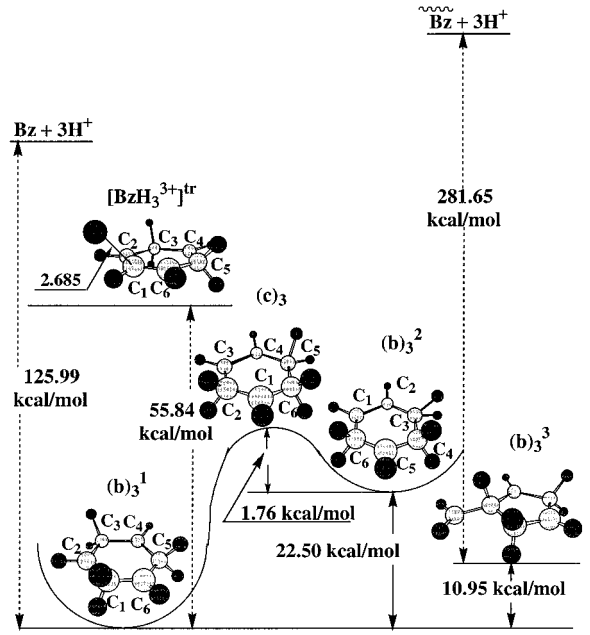

Figure 4. Lower-energy portion of the potential energy surface of the triprotonated benzene. Bond lengths in Å. Dashed arrows indicate the unscaled relative energy difference.

TABLE 5: Geometries of the Extremum-Energy Structures Residing on the Lower-Energy Portion of the PES of the Triprotonated Benzene Molecule[a]

geometry	$(b)_3^1$	$(b)_3^2$	$(c)_3$	$(b)_3^3$
$r(C_1C_2)$	1.461	1.472	1.472	1.463
$r(C_2C_3)$	1.461	1.379	1.423	1.557
$r(C_3C_4)$	1.461	1.497	1.511	1.449
$r(C_4C_5)$	1.461	1.444	1.392	1.474
$r(C_5C_6)$	1.461	1.460	1.507	1.447
$r(C_6C_1)$	1.461	1.444	1.431	1.498
$r(C_1H_1)$	1.102	1.101	1.101	1.102
$r(C_2H_2)$	1.136 (+0.810)[b]	1.097	1.152	1.167
$r(C_3H_3)$	1.102	1.226 (+0.512)[b]	1.102	1.114
$r(C_4H_4)$	1.136 (+0.810)[b]	1.129 (+0.843)[b]	1.099	1.101
$r(C_5H_5)$	1.102	1.101	1.143	1.137
$r(C_6H_6)$	1.136 (+0.810)[b]	1.144 (+0.784)[b]	1.124	1.102
r(CH)[c]	1.136 (−0.810)[b]	1.226 (−0.512)[b]	1.153	1.102
r(CH)[c]	1.136 (−0.810)[b]	1.129 (−0.843)[b]	1.202	1.123
r(CH)[c]	1.136 (−0.810)[b]	1.144 (−0.784)[b]	1.138	1.137

[a] For enumeration of the atoms see Figure 4. Bond lengths in Å. The superscript *b* indicates the distance above (+) and below (−) the Bz ring, respectively, and *c* the C−H bonds with the residing excess protons.

and below the dissociation limit (d) + H^+ by 46.7 kcal/mol and is composed of H_2 diatom with Mulliken charges 0.04 and 0.05 separated by a distance of 0.743 Å. Its bond axes lies perpendicular to the loosely bounded C−H bond directed toward its midpoint at a distance of ca. 2.1 Å from the hydrogen atom residing above the Bz ring by 22.7°. The corresponding ν(H−H) stretching vibration is predicted at 4536 cm^{-1} (see Table 3).

5. Triprotonated Benzene

The lower energy portion of the PES of triprotonated benzene shown in Figure 4 consists of three energy minima linked with each other by two transition structures. The global minimum energy structure $(b)_3^1$ of BzH_3^{3+} is of the C_{3v} symmetry with the ∠HCH = 91.2° and the C−H bond length of 1.136 Å at the protonation sites (see Table 5). Compared with the (o) structure, its C−H stretching vibrations at the protonation sites are further red shifted by ∼150 cm^{-1} and some of them are enhanced by a factor of nearly 2 (Table 3). Structure $(b)_3^1$ lies below the asymptote Bz + $3H^+$ by ∼125.99 kcal/mol which is less than the proton affinity of benzene by 47.3 kcal/mol. This implies that $(b)_3^1$ is unstable relative to the stable mono- and diprotonated Bz, and thus the triprotonation of bare benzene may occur via its simultaneous protonation by three excess protons or by protonation of the diprotonated Bz or by its diprotonation. In the former case, the product structure becomes stable whereas in latter cases, it has a finite lifetime determined by the activation barrier separating the product from the reactants.

Consider now the nonsymmetric minimum-energy structure $(b)_3^2$ displayed in Figure 4 and lying by 22.50 kcal/mol above $(b)_3^1$. It has three different C−H bonds at the protonation sites varying from 1.129 and 1.226 Å for the two nearest-neighbor protonation sites to 1.144 Å for the other site. This is demonstrated in Table 5. A simultaneous double-proton migration between $(b)_3^1$ and $(b)_3^2$ is governed by the transition structure $(c)_3$, which is placed energetically rather close to the structure $(b)_3^2$, by about 1.76 kcal/mol. In other words, the structure $(b)_3^2$ is likely unstable relative to the symmetric triprotonated structure of BzH_3^{3+}. The transition structure $(c)_3$ is characterized by a single imaginary frequency of 555 cm^{-1}, describing the out-of-plane migration of one excess proton shared by the two adjacent carbon atoms.

The transition state $[BzH_3^{3+}]^{tr}$ lies by 135.22 kcal/mol higher than the dissociative limit BzH_2^{2+} + H^+. It is similar to the $[BzH^+]^{tr}$ structure discussed in section 3, and its activation barrier, characterized by the imaginary frequency of 755 cm^{-1}, controls the lifetime of the protonated products relative to the aforementioned dissociative limit. In $[BzH_3^{3+}]^{tr}$, the excess proton approaches the ortho diprotonated benzene (o) and resides at a distance of 2.685 Å to the nearest carbon atom of the (o) structure, forming the angle of 57.2° with its C−H bond. $[BzH_3^{3+}]^{tr}$ separates the reactant channel BzH_2^{2+} + H^+ from the two minimum-energy structures. The lowest one of them is actually the structure $(b)_3^1$ lying below it by 55.84 kcal/mol, which has a finite lifetime relative to this reactant dissociative limit. The one is, by analogy with section 3, a van der Waals complex formed by the diprotonated vdW complex and H^+.

On the lower-energy portion of the PES of triprotonated benzene, we also locate the minimum-energy structure $(b)_3^3$, which is actually the diprotonated structure (b) and is higher in energy by 10.95 kcal/mol relative to $(b)_3^1$. On the other hand, with respect to the dissociation limit $\widetilde{Bz}$ + $3H^+$, $(b)_3^3$ lies below by 299.43 kcal/mol which reduces to 281.65 kcal/mol after ZPVE. Its geometry is presented in Table 5 and, as demonstrated in Figure 2, it is composed of the diprotonated cyclopentadienyl unit with the bonded CH_2 group leaned out of the cyclopentadienyl ring by 153° and causes the rotation of the C_2−H_2 bond by 90° relative to the same ring. The C−H stretching of the $(b)_3^3$ complex is displayed in Figure 2. Its rotational constants take the following values: A = 6822.4916, B = 3275.2914, and C = 23405.050 MHz.

6. Tetra Protonation of Benzene

The tetra protonation reaction of bare benzene has two channels shown in Figure 5. In both channels, the products are energetically less favored compared to Bz. One channel leads to opening of the Bz ring, $(b)_4^1$. Their energy difference amounts to 62.38 kcal/mol. The other one ends at the structure $(b)_4^2$ interpreted as a doubly protonated para structure. It is

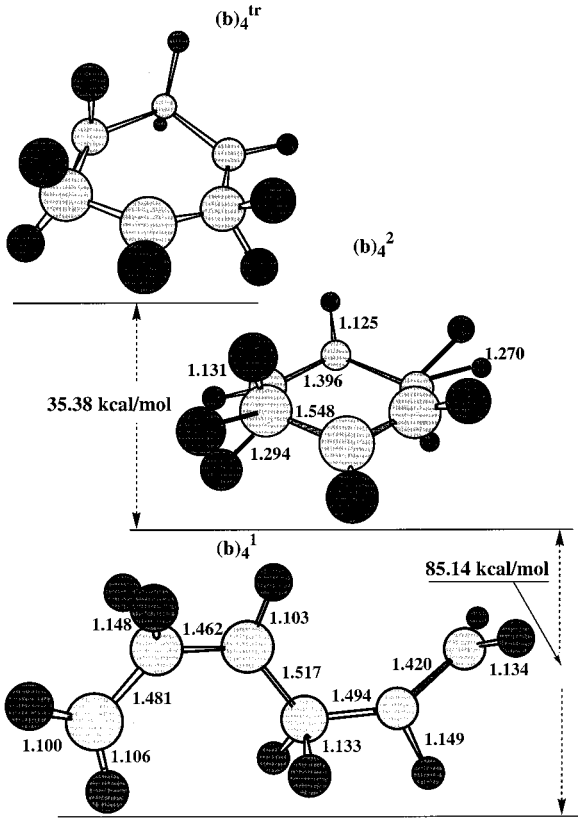

Figure 5. Tetra protonation of benzene. Bond lengths in Å. Dashed arrows indicate the unscaled relative energy difference.

worth mentioning that it possesses two partly charged hydrogen atoms on the opposite carbons residing rather closer, by 0.950 Å, to each other.

The transition structure $(b)_4^{tr}$ that actually preopens the benzene ring is a saddle point of second-order lying rather high, by 120.52 kcal/mol, above the product limit. At this stage, the benzene ring is preopened at a rather long C_1-C_2 bond with the length of 1.662 Å. The structure $(b)_4^{tr}$ is characterized by two imaginary frequencies 851 and 289 cm^{-1}, both describing the asymmetric C−C stretching vibration of the C_1-C_2 bond coupled to the vibrations of the CH_2 group placed at its ends.

7. Conclusions and Outlook

We have performed a rather exhaustive search of the lower energy portion of the PES of the reaction $Bz + H^+$ and shown that (i) the benzenium cation exists as the canonical C_{2v} conformer (b) of the σ-type bonding; (ii) the $(\tilde{b})$ structure, which is less stable than (b) by 18.14 kcal/mol, exists in the reactions of protonation of tricylic conformer $\widetilde{Bz}$ of Bz; (iii) the PA of $\widetilde{Bz}$ exceeds the PA of Bz by nearly 44 kcal/mol; (iv) on the PES of BzH^+, there exists the transition structure $[BzH^+]^{tr}$ governing the transition between a van der Waals complex and (b); (v) we have determined two structures (d) and $(d)^{saddle}$ that underlie the reaction channel (2) on the PES of BzH^+ related to the H_2 loss.

The structure composed of H_2 and $C_6H_5^+$ appears to be rather unstable and short-lived, and therefore, it seems rather difficult to explain the mass spectrometry experiments on the collision-induced dissociation of the monoprotonated Bz into the product channels involving H and H_2. It might be possible to interpret these experiments in terms of simultaneous mono- and diprotonations of Bz because, as we have found, the diproton affinity of Bz is higher than the first one by 36.9 kcal/mol. We envisage the collision-induced dissociation of the mono- and diprotonated benzene as follows. The first dissociation channel related to the H loss starts at the global minimum structures of the (b) and (m) types. The second one ending particularly at the H-2 product starts from the diprotonated structure, $(d)_2^1$.

In the context of the present work, it is quite interesting to make a comparison of the positive multiply charged complexes with the analogous negatively charged ones. In the latter case, there exists a strong Coulomb repulsion between the excess negative charges resulting in the appearance of the enormous repulsive Coulomb barrier that makes, for instance, many diatomic and triatomic dianions unstable.[18] In contrast, as we have shown in the present work on the multiprotonation of benzene, it admits di- and even triprotonation leading both to the stable structures, whereas the tetra one destabilizes it by opening the Bz ring and results in diprotonated hexa-1,3,5-triene. However, it is worth mentioning that the triprotonation of benzene must proceed simultaneously. That is why it is rather intriguing to study a simultaneous attack of neutral molecules by, for example, a pair of electrons where we can apparently expect a lowering of their Coulomb repulsion (see, e.g., ref 19 for the two-electron attachment to He_2^+).

Acknowledgment. One of the authors, R.S., acknowledges Alexander von Humboldt Stiftung for the financial support and Sigrid D. Peyerimhoff for her warm hospitality. E.S.K. acknowledges Grant of the Katholiek University Leuven and thanks Thérèsa Zeegers-Huyskens and Minh Tho Nguyen for fruitful discussions and warm hospitality. We also thank the referees for valuable suggestions and comments.

Appendix: Benzene Conformer $\widetilde{Bz}$

Figure 2 displays the tricylo[4.1.1.0]hexan-3-ene, $\widetilde{Bz}$, an isomer of benzene, and its harmonic C−H stretching vibrations. Protonation of $\widetilde{Bz}$ results in $(\tilde{b})$. $\widetilde{Bz}$ is higher compared to Bz by 72.79 kcal/mol, which is reduced to 70.19 kcal/mol after ZPVE. It is interesting, in this context, to compare this energy difference with that found between (b) and $(\tilde{b})$ (18.14 kcal/mol), their protonated analogues. In other words, the protonation of these species decreases their energy difference by a factor of nearly 4.

In contrast to the nonpolar Bz molecule, $\widetilde{Bz}$ possesses a total dipole moment of 0.98 D. Its diagonal quadrupole moments are also worth mentioning too: $Q_{xx} = 33.69$ (31.90) D·Å, $Q_{yy} = 32.74$ (31.90) D·Å, and $Q_{zz} = 38.67$ (41.47) D·Å, and compare with those of Bz given in parentheses. Finally, the theoretical rotational constants of the $\widetilde{Bz}$ conformer are the following: $A = 7367.4074$ MHz, $B = 5272.9643$ MHz, and $C = 3888.4149$ MHz.

References and Notes

(1) (a) Olah, G. A. *Acc. Chem. Res.* **1971**, *4*, 240. (b) Olah, G. A.; Prakash, G. K. S.; Sommer, J. *Superacids*; Wiley: New York, 1985 and references therein. (c) Olah, G. A.; Schlosberg, R. H.; Porter, R. D.; Mo, Y. K.; Kelly, D. P.; Mateescu, G. D. *J. Am. Chem. Soc.* **1972**, *94*, 2034. (d) Olah, G. A.; Staral, J. S.; Asencio, G.; Liang, G.; Forsyth, D. A.; Mateescu, G. D. *J. Am. Chem. Soc.* **1978**, *100*, 6299.

(2) (a) de la Mare, P. B. D.; Bolton, R. *Electrophilic Addition to Unsaturated Systems*; Elsevier: Amsterdam, 1982. (b) Perkampus H.-H.; Baumgarten, E. *Angew. Chem., Int. Ed. Engl.* **1964**, *3*, 776. (c) Koptyug, V. A. *Top. Curr. Chem.* **1984**, *122*, 1. (d) Lau Y. K.; Kebarle, P. *J. Am. Chem. Soc.* **1976**, *98*, 7452.

(3) (a) Mason, R. S.; Williams, C. M.; Anderson, P. D. J. *J. Chem. Soc., Chem. Commun.* **1995**, 1027. (b) Somogyi, A.; Kane, T. E.; Ding, J.-M.; Wysocki, V. H. *J. Am. Chem. Soc.* **1993**, *115*, 5275. (c) Kuck, D. *Mass Spectrom. Rev.* **1990**, *9*, 187. (d) Kuck, D. *Mass Spectrom. Rev.* **1990**,

9, 583. (e) Laali, K. K. *Chem. Rev.* **1996**, *96*, 1873. (f) Fornarini, S. *Mass Spectrom. Rev.* **1996**, *15*, 365. (g) Chiavarino, B.; Crestoni, M. E.; Fornarini, S.; DePuy, C. H.; Gareyev, R. *J. Phys. Chem.* **1996**, *100*, 16201. (h) DePuy, C. H.; Gareyev, R.; Fornarini, S. *Int. J. Mass Spectrom. Ion Proc.* **1997**, *161*, 43. (i) Fornarini, S.; Crestoni, M. E. *Acc. Chem. Res.* **1998**, *31*, 827. (j) Kuck, D. *Angew. Chem., Int. Ed. Engl.* **2000**, *39*, 125.

(4) Alder, R. W.; Baker, R.; Brown, J. M. *Mechanisms in Organic Chemistry*; Wiley: New York, 1971.

(5) (a) Streitwieser, A.; Heathcock, C. H. *Introduction to Organic Chemistry*; Macmillan: New York, 1981. (b) See also Wang, D. Z.; Streitwieser, A. *Theor. Chem. Acc.* **1999**, *102*, 78.

(6) Hehre, W. J.; Radom, L.; Schleyer, P. v. R.; Pople, J. A. *Ab Initio Molecular Orbital Theory*; Wiley: New York, 1986.

(7) Sundaralingham, M.; Chwang, A. K. In *Carbonium Ions*; Olah, G. A., Schleyer, P. v. R., Eds.; Wiley: New York, 1976; Vol. 5, p 2427.

(8) (a) Chong, S. L.; Franklin, J. L. *J. Am. Chem. Soc.* **1972**, *94*, 6630. (b) Haney, M. A.; Franklin, J. L. *J. Phys. Chem.* **1969**, *73*, 4328. (c) Aue, D. H.; Bowers, M. T. In *Gas Phase Ion Chemistry*; Bowers, M. T., Ed.; Academic: New York, 1979; Vol. 2, p 1. (d) Szulejko, J. E.; McMahon, T. B. *J. Am. Chem. Soc.* **1993**, *115*, 7839. (e) Hunter, E. P.; Lias, S. G. *J. Phys. Chem. Ref. Data* **1998**, *27*, *3*, 413.

(9) (a) Muller, N.; Pickett, L. W.; Mulliken, R. S. *J. Am. Chem. Soc.* **1954**, *76*, 4770. (b) Heglstand, E. *Acta Chem. Scand.* **1970**, *24*, 3687. (c) Jakubetz, W.; Schuster, P. *Angew. Chem., Int. Ed. Engl.* **1971**, *10*, 497. (d) Hehre, W. J.; Pople, J. A. *J. Am. Chem. Soc.* **1972**, *94*, 6901. (e) Ermler, W. C.; Mulliken, R. S.; Clementi, E. *J. Am. Chem. Soc.* **1976**, *98*, 388.

(10) (a) Köhler, H.-J.; Lischka, H. *J. Am. Chem. Soc.* **1979**, *101*, 3479. (b) Bader, R. F. W.; Chang, C. *J. Phys. Chem.* **1989**, *93*, 5095. (c) Howard, S. T.; Wozniak, K. *Chem. Phys. Lett.* **1993**, *212*, 1. (d) Calef, B.; Redondo, A. *Chem. Phys. Lett.* **1994**, *223*, 1. (e) Glukhovtsev, M. N.; Pross, A.; Nicolaides, A.; Radom, L. *J. Chem. Soc., Chem. Commun.* **1995**, 2347. (f) Sieber, S.; Schleyer, P. v. R.; Gauss, J. *J. Am. Chem. Soc.* **1993**, *115*, 6987. (g) Maksič, Z. B.; Kovačević, B.; Lesar, A. *Chem. Phys.* **2000**, *253*, 59. (h) Del Rio, E.; López, R.; Sordo, T. L. *J. Phys. Chem. A* **1997**, *101*, 10090.

(11) Vékely, K. *Mass Spectrom. Rev.* **1995**, *14*, 195.

(12) *GAUSSIAN 98* (Revision A.9); Frisch, M. J.; Trucks, G. W.; Schlegel, H. B.; Scuseria, G. E.; Robb, M. A.; Cheeseman, J. R.; Zakrzewski, V. G.; Montgomery, J. A., Jr.; Stratmann, R. E.; Burant, J. C.; Dapprich, S.; Millam, J. M.; Daniels, A. D.; Kudin, K. N.; Strain, M. C.; Farkas, O.; Tomasi, J.; Barone, V.; Cossi, M.; Cammi, R.; Mennucci, B.; Pomelli, C.; Adamo, C.; Clifford, S.; Ochterski, J.; Petersson, G. A.; Ayala, P. Y.; Cui, Q.; Morokuma, K.; Malick, D. K.; Rabuck, A. D.; Raghavachari, K.; Foresman, J. B.; Cioslowski, J.; Ortiz, J. V.; Baboul, A. G.; Stefanov, B. B.; Liu, G.; Liashenko, A.; Piskorz, P.; Komaromi, I.; Gomperts, R.; Martin, R. L.; Fox, D. J.; Keith, T.; Al-Laham, M. A.; Peng, C. Y.; Nanayakkara, A.; Challacombe, M.; Gill, P. M. W.; Johnson, B.; Chen, W.; Wong, M. W.; Andres, J. L.; Gonzalez, C.; Head-Gordon, M.; Replogle, E. S.; Pople, J. A. Gaussian, Inc.: Pittsburgh, PA, 1998.

(13) (a) Plíva, J.; Johns, J. W. C.; Goodman, L. *J. Mol. Spectrosc.* **1991**, *148*, 427. (b) Handy, N. C.; Maslen, P. E.; Amos, R. D.; Andrews, J. S.; Murray, C. W.; Laming, G. J. *Chem. Phys. Lett.* **1992**, *197*, 506. (c) Goodman, L.; Ozkabak, A. G.; Thakur, S. N. *J. Phys. Chem.* **1991**, *95*, 9044. (d) Palafox, M. A. *Int. J. Quantum Chem.* **2000**, *77*, 661. (e) In ref. 13d, this ν(C═C) stretching vibration is assigned to the B_{2u} symmetry.

(14) The reaction path data from the transition state $[BzH^+]^{tr}$ to the (b) structure and towards the vdW one are available on request. We were unable to locate the vdW complex at the MP2(full)/6-311++G(d,p) computational level.

(15) (a) Gleghorn, J. T.; McConkey, F. W. *J. Chem. Soc., Perkin Trans. 2* **1976**, 1078. (b) Sordo, T.; Bertrán, J.; Canadell, E. *J. Chem. Soc., Perkin Trans. 2* **1979**, 1486.

(16) Kryachko, E. S.; Nguyen, M. T. *J. Phys. Chem. A* **2001**, *105*, 153.

(17) Huber, K. P.; Herzberg, G. *Molecular Spectra and Molecular Structure Constants of Diatomic Molecules*; Van Nostrand Reinhold: New York, 1979.

(18) (a) Scheller, M. K.; Compton, R. N.; Cederbaum, L. S. *Science* **1995**, *270*, 1160. (b) Sommerfeld, T.; Riss, U. V.; Meyer, H.-D.; Cederbaum, L. S. *Phys. Rev. Lett.* **1997**, *79*, 1237 and references therein.

(19) Bacalis, N. C. *J. Phys. B: Atom. Mol. Opt. Phys.* **2000**, *33*, 1415.